JOURNAL OF MATERIALS SCIENCE 28 (1993) 2157–2162

Thermal decomposition of Mg, Al-hydrotalcite material

M. L. VALCHEVA-TRAYKOVA, N. P. DAVIDOVA
Institute of Kinetics and Catalysis, Bulgarian Academy of Sciences, G. Bonchev Street 11, 1140 Sofia, Bulgaria

A. H. WEISS
Department of Chemical Engineering, Worcester Polytechnic Institute, 100 Institute Road, Worcester, MA 01609, USA

The effect of by-products obtained during the low-temperature synthesis of Mg, Al- hydrotalcite on further thermal decomposition of hydrotalcite material was studied by X-ray powder diffraction, scanning electron microscopy, transmission electron microscopy and infrared spectroscopy. By-products, which thermally decomposed below 450 °C, led to the formation of α-Al_2O_3 and MgO; by-products which completely decomposed above 500 °C resulted in the formation of $MgAl_2O_4$ and a sharp increase in MgO dispersity.

1. Introduction

Hydrotalcites are a large group of natural and synthetic clay minerals of brucite-like structure [1–4]. Thermally decomposed hydrotalcite materials have been used as catalysts for several chemical reactions taking place between 300 and 1000 °C [5–15].

Simultaneous to the formation of hydrotalcite, the formation of some by-products was observed under low-temperature synthesis conditions [16–18], some of which may be amorphous, highly dispersed, or may be found in small amounts. Following their detection, it became necessary to overcome the problems of the limitations of the method and to verify their presence using different techniques.

The effect of by-products on the transformations during heat treatment of hydrotalcite material were not completely investigated. According to several studies [19–21] only Me(II)O and/or finely dispersed Al_2O_3 matrix was detected after thermal decomposition of hydrotalcite material above 300 °C, while other studies [14–18] showed a mixture of Me(II)O and Me(II) $Me(III)_2O_4$.

The purpose of the present work was to study the effect of some by-products on the composition of thermally degraded hydrotalcite material. A combination of physical methods was selected, in order to be able to investigate more completely the composition of the starting material and its relative changes during heat treatments.

2. Experimental methods

Mg, Al-hydrotalcite material was synthesized by a low-temperature procedure, as described previously [9]. X-ray diffraction (XRD) analysis of this material was performed using a General Electric XRD-5 X-ray diffraction unit, at CuK_α irradiation in the range $2\theta = 5–50°$. Scanning electron micrographs were recorded using a Toshiba "T-200" apparatus at electron microscopic magnifications of 1000, 3500, 5000 and 10000, and a photographic magnification of 2×1. Samples were prepared as described earlier [11–13]. Transmission electron micrographs were recorded on a "JEM-100 B" apparatus, $U = 80$ kV, at electron microscopic magnifications of 20000, 30000, 35000, 50000, 60000, 70000, 80000 and photographic magnification 4×1. Samples were prepared for TEM investigations as described elsewhere [6, 22]. Infrared spectra were recorded on a Bruker "IFS 113 V" Fourier transform infrared spectrometer in the range 4000–400 cm^{-1} (standard error of $\pm$ 1 cm^{-1}), in KBr tablets, in air.

3. Results

3.1. X-ray powder diffraction

The XRD pattern of the uncalcined material is shown in Fig. 1. Reflections of Mg, Al-hydrotalcite, manasseite, indiperite and gibbsite were detected [23]; those of indiperite and gibbsite were very weak and diffuse.

In the XRD pattern of 300 °C-calcined material, the reflections of hydrotalcite, gibbsite and indiperite were absent and those of manasseite became very weak and diffuse. Simultaneously, weak and diffuse reflections of α-Al_2O_3, MgO and dipinite [23] appeared.

The disappearance of hydrotalcite reflections and the decrease in manasseite are probably related to the formation of finely dispersed phases of MgO and α-Al_2O_3, as pointed out elsewhere [18]. The total thermal decomposition of hydrotalcite and manasseite was accompanied by the highest increase in intensity of the MgO reflection. Evidently, MgO was formed by thermal decomposition of these two compounds. It was also shown that the presence of manasseite in our

0022–2461

case had no influence on the phase transitions during heat treatment at this temperature. The appearance of dipinite reflections may be attributed to the thermal decomposition of indiperite. The complete thermal decomposition of indiperite at about 500–600 °C was accompanied by the appearance of spinel ($MgAl_2O_4$) reflections in the XRD pattern (Fig. 2, curve 3).

During heat treatment above 400 °C, α-Al_2O_3 began to appear, together with MgO. The evolution of CO_2 in the heat treatment at above 450 °C was expected to cause an increase in the dispersion of some components. Fig. 2 gives grounds to assume that redispersion will concern MgO. Evidence may be found on the basis of SEM and TEM data.

3.2. Scanning electron microscopy

Scanning electron micrographs of uncalcined material (Fig. 3a) showed very well crystallized hydrotalcite, magnesium–aluminum hydroxycarbonates, small amounts of boehmite and gibbsite crystals. Fine granular amorphous material is seen on the crystal walls and edges (Fig. 3b). The fact that boehmite is invisible in the X-ray diffraction pattern (Fig. 1) may be related to its small amount in the sample. The amorphous fine granular mass, seen in Fig. 3b, is most

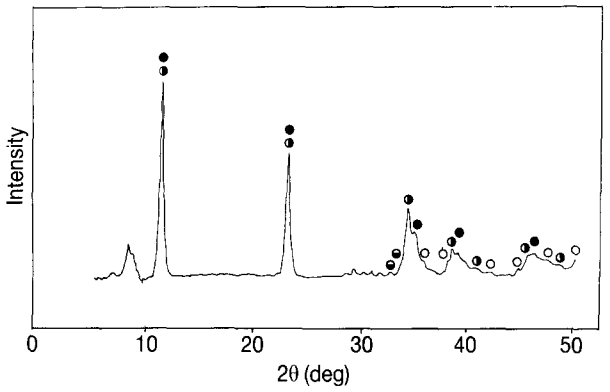

Figure 1 X-ray diffraction pattern of the uncalcined Mg, Al-hydrotalcite material: (○) gibbsite, (○) indiperite, (●) hydrotalcite, (◑) manasseite.

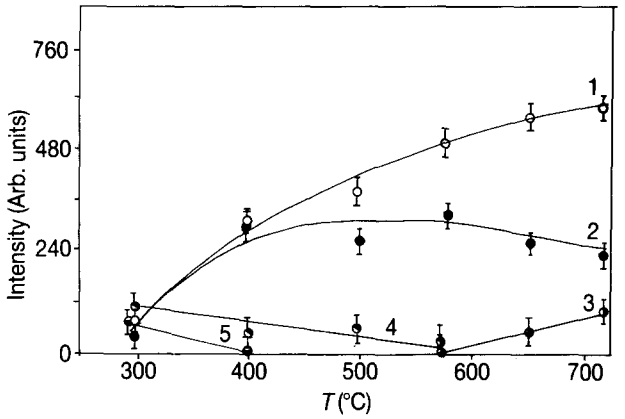

Figure 2 Relative changes in intensity of the characteristic XRD reflections of (1) α-Al_2O_3, (2) MgO, (3) $MgAl_2O_7$, (4) $5 \cdot MgO \cdot 4CO_3 \cdot 6H_2O$, (5) $Mg_2Al_2(OH)_{10} \cdot CO_3 \cdot 4H_2O$ during calcination of the Mg, Al-hydrotalcite material.

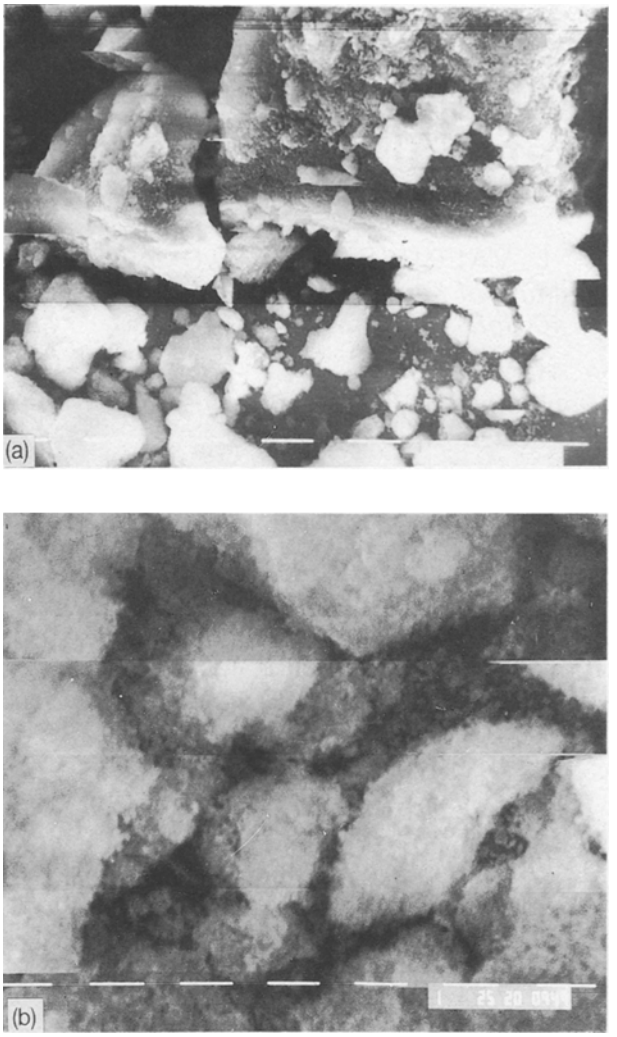

Figure 3 Scanning electron micrographs of the uncalcined Mg, Al-hydrotalcite material at (a) × 1000 and (b) × 10 000.

probably gibbsite. This assumption is in agreement with the very weak and diffuse reflections of $Al(OH)_3$ in the XRD pattern of the uncalcined material (Fig. 1).

After treatment at 725 °C, significant changes in the sample were observed (Fig. 4). Fine granular masses were located on the walls of the well-shaped crystals of α-Al_2O_3 and $MgAl_2O_4$. Crystals of MgO, α-Al_2O_3 and spinel were seen (Fig. 4a). MgO crystals had porous walls and uneven edges (Fig. 4b). According to other authors [20, 21], finely dispersed particles seen in Fig. 4c, should be of amorphous Al_2O_3. The chemical nature of the highly dispersed phase in our case was elucidated on the basis of TEM and infrared data.

3.3. Transmission electron microscopy

Along with single-crystal bodies (Fig. 5a) and concretions (Fig. 5c) of hydrotalcite, concretions of hydrotalcite entrained in aluminium hydroxides (Fig. 5b), and crystal concretions of Mg, Al-hydroxycarbonates (Fig. 5c) were also observed. Fig. 5d shows a crystal concretion of Mg, Al-hydroxycarbonates in close vicinity to hydrotalcite and gibbsite.

In the transmission electron micrographs of the calcined material, α-Al_2O_3 (Fig. 6a), MgO crystals in the α-Al_2O_3 matrix (Fig. 6b), MgO crystals in the

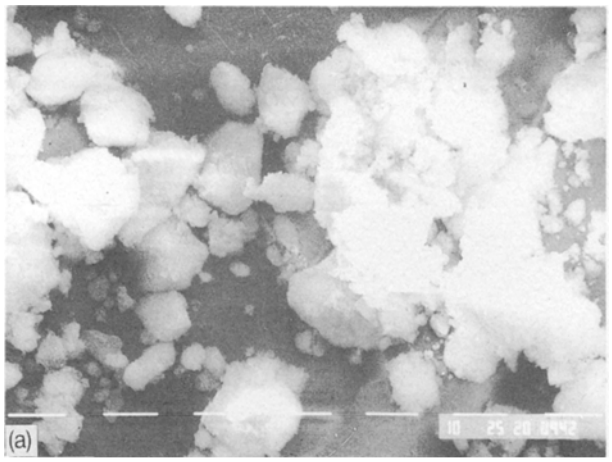

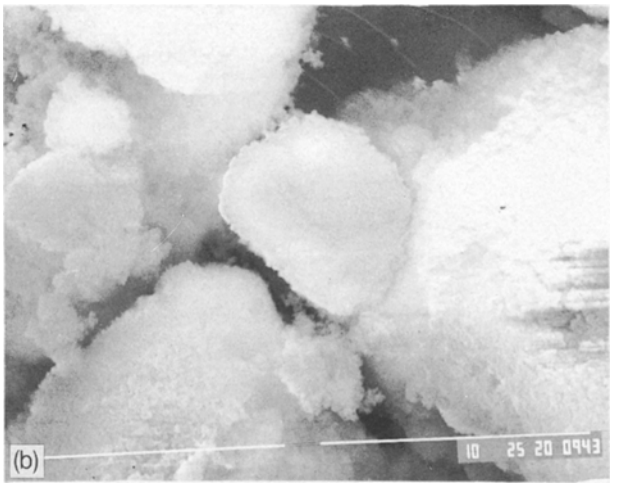

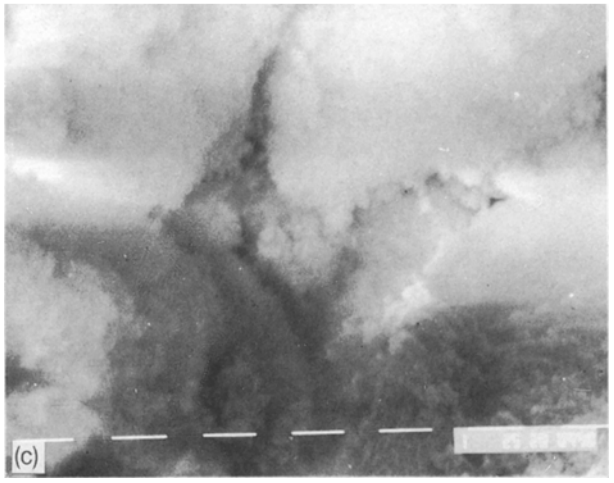

Figure 4 Scanning electron micrographs of the Mg, Al-hydrotalcite material after heat treatment at 725 °C (a) × 1000 (b) × 5000 and (c) × 10 000.

highly dispersed MgO matrix (Fig. 6c), and particles of $MgAl_2O_4$ in the highly dispersed MgO matrix (Fig. 6d), can be distinguished.

These results confirm fully the XRD and SEM data on phase compositions of uncalcined and calcined materials. Moreover, they show that the finely dispersed phase observed in the scanning electron micrographs of the calcined material was MgO and not Al_2O_3.

3.4. Infrared spectroscopy

In the infrared spectrum of the uncalcined sample (Fig. 7a) an intense and sharp characteristic band at 451 cm^{-1} was observed. According to other authors [22, 24, 25] it could be characteristic of condensed $[AlO_6]^{3-}$ groups as well as of single groups with an Al_{oh}–O bond length of 0.161 nm, which is typical for hydrotalcites [17, 21, 26, 27, 30–32]. The bond observed at 555 cm^{-1} may be related to a superposition of deformational vibrations of Me^{n+}–OH^- bonds in $[Me^{n+}(OH)_x]^{n-x}$ ($x = 6$) [16, 17, 23, 24, 31], with bond length 0.203–0.204 nm in hydrotalcite [16, 17], manasseite and/or Al_2O_3 [23]. The broad band at 663 cm^{-1} (Fig. 7a) most probably is a superposition of the characteristic bonds of boehmite, hydrotalcite and manasseite in this frequency interval [7, 15, 16, 19]. The doublet at 791, 663 cm^{-1} coincides by position and intensity ratio with the corresponding characteristic vibrations of hydrotalcite [17]. The rather broad band at 960–945 cm^{-1} may be related to a superposition of characteristic vibrations for hydrotalcite [17] and gibbsite [23]. The shoulder at about 850 cm^{-1} is typical for boehmite (AlOOH) [23], while the weak one at 1020 cm^{-1} may be assigned to the gibbsite vibration [23]. Two very intense bands observed at 1367 cm^{-1}, 1383 cm^{-1} and a weak broad one at 1579 cm^{-1}, may undoubtedly be related to the characteristic vibrations of CO_3^{2-} groups [16, 17, 28, 35–37]. By analogy with Mg^{2+}–CO_3^{2-} [29, 34], the band at 1367 cm^{-1} may be referred to a structural vibration of the Al^{3+}–CO_3^{2-} bond in the Mg, Al-hydroxycarbonates, and in Mg, Al-hydrotalcite [18, 34–37]. The band at 1383 cm^{-1} may be referred to CO_3^{2-}–H_2O vibrations [28]. The broad band of medium intensity at 1579 cm^{-1} is probably a result of the HO . . .OH (d = 0.284 nm), HO . . .CO_3^{2-} (d = 0.29 nm) and H_2O . . .CO_3^{2-} (d = 0.271 and 0.350 nm) [16, 18]. The intense broad band observed between 4000 and 2700 cm^{-1} in the infrared spectrum of the uncalcined material may be represented as a superposition of deformational vibrations of physically adsorbed water [24], vibrations of structural OH^- groups [23], characteristic valent vibrations of HO . . .OH (d = 0.27 nm), and/or CO_3^{2-}–OH^- (d = 0.275 nm) in hydrotalcite [17, 23] and of characteristic stretching vibrations of the Mg^{2+}–OH^- bond in Mg, Al-hydroxycarbonates [15, 17, 23, 24].

After calcination of Mg, Al-hydrotalcite material at 725 °C, significant changes in the infrared spectrum of the sample were observed (Fig. 7b). Between 450 and 400 cm^{-1} a band appeared which is a superposition of the characteristic stretching bands of MgO and α-Al_2O_3 in this frequency interval. A broad and intense peak at 656 cm^{-1} with several shoulders (1092–1061, 955, 860–796 and 545 cm^{-1}) was detected. It is built up by the characteristic vibrations of MgO [30, 36], Al_2O_3 [30–32], and $MgAl_2O_4$ [32]. The shoulder at 1385 cm^{-1} observed is characteristic for O–C–O vibrations in the adsorbed CO_3^{2-} groups on the surfaces of the oxide system [36, 37]. The band

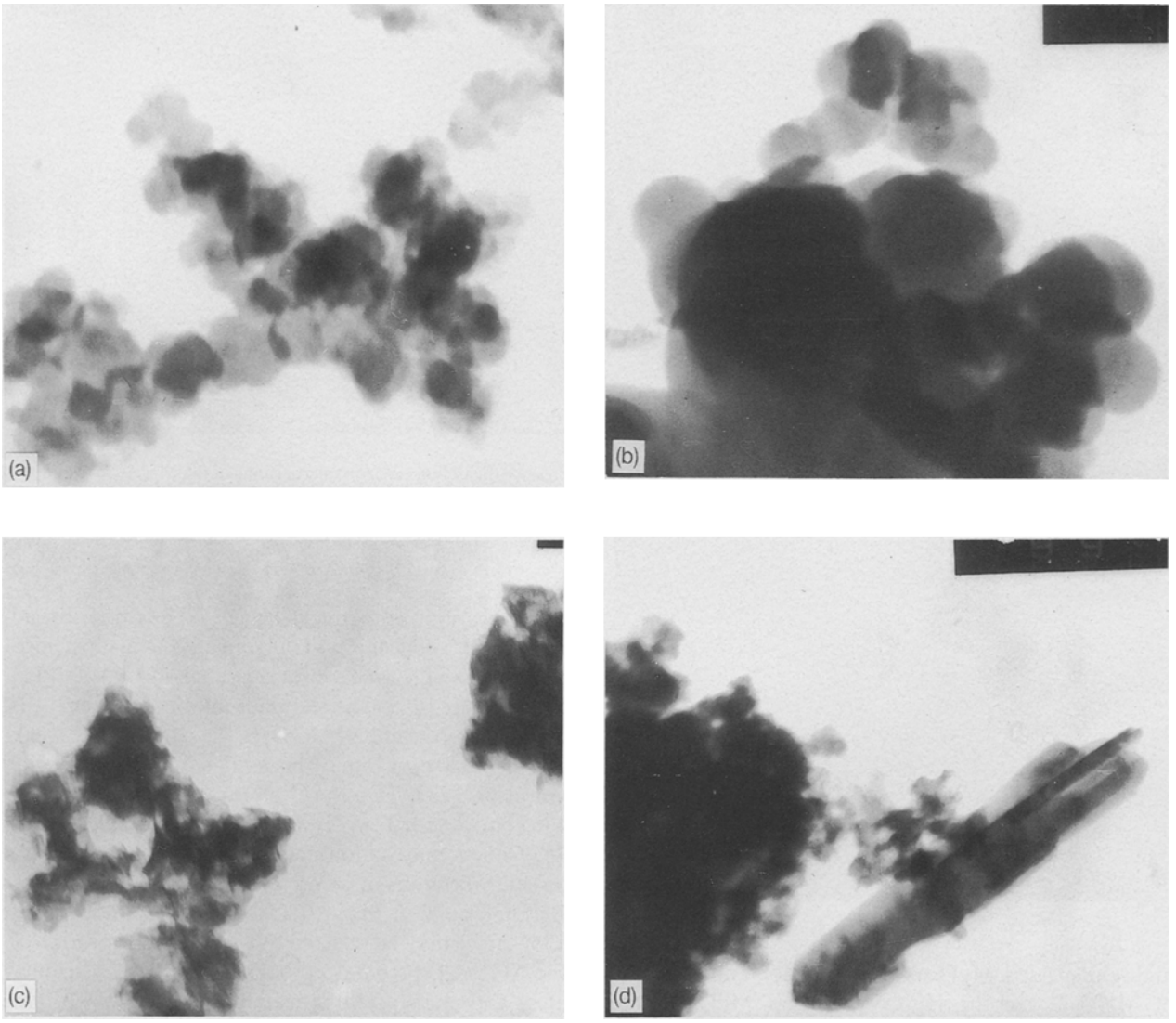

Figure 5 Transmission electron micrographs of the uncalcined Mg, Al-hydrotalcite material: (a) hydrotalcite (× 35 000), (b) hydrotalcite and gibbsite (× 60 000), (c) Mg, Al-hydroxycarbonates (× 35 000), (d) hydrotalcite, Mg, Al-hydroxycarbonates and $Al(OH)_3$ (× 35 000).

at 1649 cm^{-1} seen in the infrared spectrum of the calcined material, according to Allegra and Ronca [24], is characteristic of the vibrations of CO_3^{2-} reversibly sorbed on MgO and for physically sorbed water. The shoulders between 1600 and 1400 cm^{-1} are characteristic of the reversibly sorbed CO_3^{2-} and H_2O on the oxide surfaces [33, 35–37]. A broad, very intense peak at 3523 cm^{-1} and a weak shoulder at about 3300–3250 cm^{-1} were also detected. They are due to the valent vibrations of HO . . .OH_2 [17], H_2O . . .OH_2 [23] and H_2O . . .CO_3H^- [16, 17, 24]. This peak strongly indicates protonic bonds HO-H . . .OH_2 [17, 24]. According to Allmann [17], it may also be the result of HO . . .OH_2 vibrations, while Roy *et al.* [23] report it to be connected with H_2O valent vibrations.

4. Discussion

Our investigations show that the composition of thermally decomposed Mg, Al-hydrotalcite depends on the nature of accompanying substances in the starting material. XRD, SEM, TEM and infrared spectroscopy studies showed that the admixture of Mg, Al-hydroxycarbonates, AlOOH and $Al(OH)_3$ in the uncalcined hydrotalcite have an influence on the composition and dispersion of the thermally degraded material. Mg, Al-hydrotalcite and manasseite decomposed to form α-Al_2O_3 and MgO between 300 and 400 °C. At 300 °C, indiperite decomposed to α-Al_2O_3 and dipinite. Aluminium hydroxides were transformed into α-Al_2O_3 between 400 and 725 °C. During thermal decomposition of dipinite above 500 °C, H_2O and CO_2 were involved. According to Ved and Jarov [20], steam promoted the formation of $MgAl_2O_4$. The presence of highly dispersed MgO in the 725 °C calcined material may be attributed to thermal decomposition of dipinite.

5. Conclusions

1. Mg, Al-hydrotalcite, synthesized using a low-temperature procedure, is accompanied by the following by-products: Mg, Al-hydroxycarbonates (manasseite, indiperite) and hydroxides (boehmite, gibbsite).

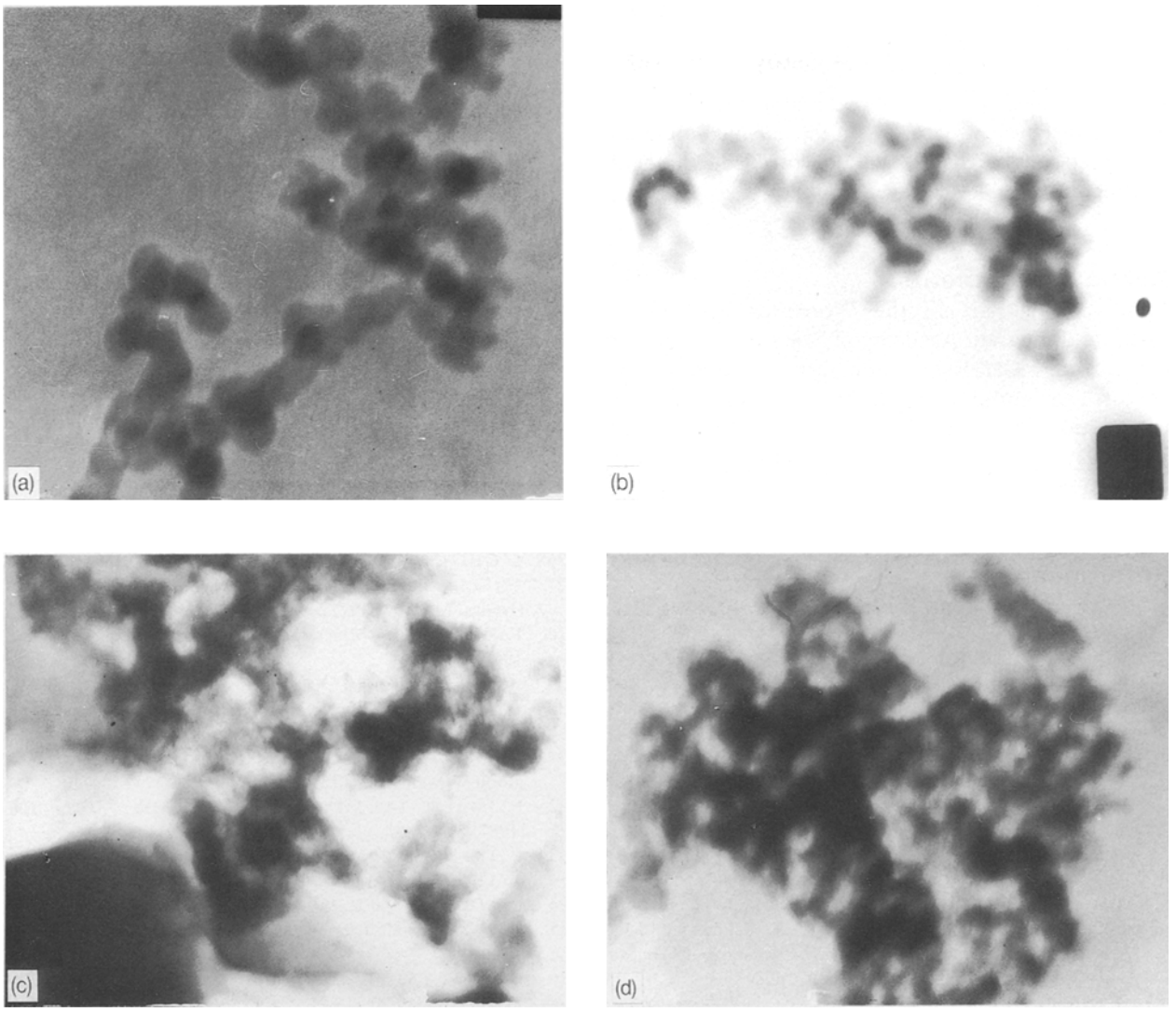

Figure 6 Transmission electron micrographs of the uncalcined Mg, Al-hydrotalcite material after heat treatment at 725 °C: (a) α-Al_2O_3 ($\times$ 60 000), (b) MgO in Al_2O_3 matrix ($\times$ 60 000), (c) MgO in amorphous MgO matrix, (d) $MgAl_2O_4$ amorphous MgO matrix.

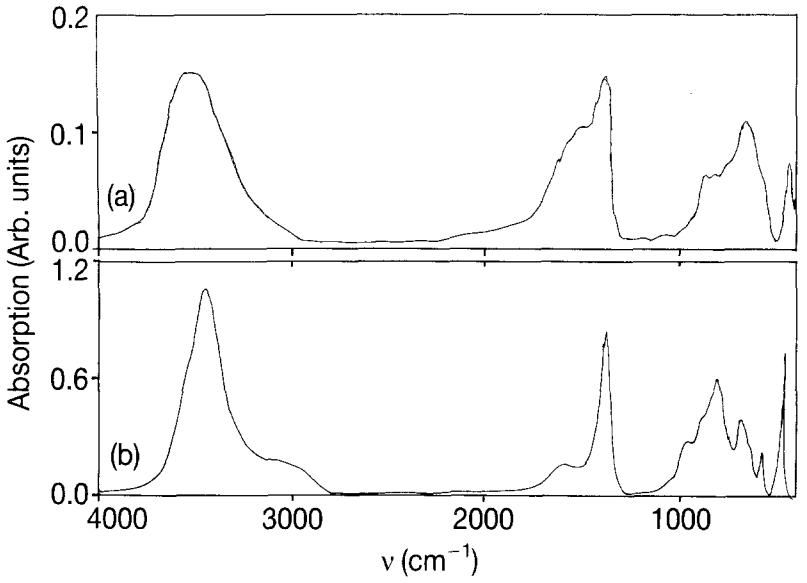

Figure 7 Infrared absorption spectra of the Mg, Al-hydrotalcite material (a) before and (b) after calcination at 725 °C.

2. After thermal decomposition of Mg, Al-hydrotalcite material at 725 °C, MgO, $MgAl_2O_4$ and α-Al_2O_3 were observed. MgO and Al_2O_3 were produced by thermal degradation of hydrotalcite and manasseite. Aluminium hydroxides and/or hydroxycarbonates thermally decomposed to α-Al_2O_3. Indiperite decomposes completely between 500 and 600 °C to form $MgAl_2O_4$.

3. The spinel formation at relatively low temperatures (between 500 and 600 °C) is related to the promoting action of steam and CO_2 released.

4. The high dispersity of MgO and the well discernible channel system observed in the calcined material are results of the effect of CO_2 evolved during heat treatment above 400 °C.

Acknowledgements

This work is part of the Worcester Polytechnic Institute–Bulgarian Academy of Sciences (Institute of Kinetics and Catalysis) Cooperative Research Program. The authors thank the National Science Foundation for financial support (Grant INT-8810539), and Lt. J. Cook for providing us with the samples of material.

References

1. R. ALLMANN and H. JEPSEN, *Neues Jb. Min. Mh.* **H12** (1969) 544.
2. L. INGRAM and H. TAYLOR, *Mineral. Mag.* **36** (1967) 465.
3. R. ALLMANN, *Acta Crystallogr.* **B24** (1968) 972.
4. *Idem, Neues Jb. Min. Mh.* **H12** (1969) 552.
5. W. REICHLE, *J. Catal.* **94** (1985) 547.
6. *Idem*, US Pat. 4 458 026 (to Union Carbide Corp., 3 July 1984).
7. S. KOHJIYA, T. SATO, T. NAKAYAMA and S. YAMASHITA, *Macromol. Chem. Rapid Commun.* **2** (1981) 231.
8. G. NATTA, in "Catalysis", edited by P. H. Emmett, III, (Reinhold, New York, (1953) Ch. 8.
9. A. H. WEISS, R. HOLMES, N. DAVIDOVA, P. KOVACHEVA and M. TRAYKOVA, in "Novel Materials in Heterogeneous Catalysis", edited by R. T. K. Baker and L. L. Murrell, ACS Symposium Series 437, (American Chemical Society, Washington, DC, 1990) Ch. 22, p. 243.
10. O. RUGERRI, F. TRIFIRO and A. VACCARI, *J. Solid State Chem.* **42** (1982) 120.
11. K. KLIER, in "Advances in Catalysis", Vol. 31, edited by D. D. Eley, H. Pines and P. B. Weisz (Academic Press, New York, 1982) p. 243.
12. P. COURTY and C. MARCILLY, in "Preparation of Catalysts III", edited by G. Poncelet, P. Grange and P. A. Jakobs (Elsevier, Amsterdam, 1983) p. 485.
13. M. ULIBARRI and H. HERNANDEZ, *Mater. Chem. Phys.* **14** (1986) 209.
14. P. GERARDI, O. RUGGERI, F. TRIFIRO, A. VACCARI, G. DEL PIWRO, G. MANARA and B. NOTARI, in "Preparation of Catalysts III", edited by G. Poncelet, P. Grange and P. A. Jakobs (Elsevier, Amsterdam, 1983) p. 723.
15. F. MUMPTON, H. JAFFE and C. THOMPSON, *Amer. Mineral.* **50** (1965) 1893.
16. F. TRIFIRO, and A. VACCARI, *J. Catal.* **85** (1985) 260.
17. R. ALLMANN, *Chimia* **24** (1970) 99.
18. T. SATO, T. WAKABAYASHI and M. SHIMADA, *Ind. Eng. Prod. Res. Dev.* **25** (1986) 89.
19. P. ROUXHET and H. TAYLOR, *Chimia* **23** (1969) 480.
20. E. VED and E. JAROV, *Ukr. Chim. J.* **37** (1971) 1017.
21. G. ROSS and H. KODAMA, *Amer. Mineral.* **52** (1967) 1036.
22. W. REICHLE, S. KANG and D. EVERHARDT, *J. Catal.* **101** (1986) 352.
23. D. ROY, R. ROY and E. OSBORN, *Amer. J. Sci.* **251** (1953) 337.
24. G. ALLEGRA, and G. RONCA, *Acta Crystallogr.* **A34** (1978) 1006.
25. S. ASBRING and L. NARRBY, *ibid.* **B26** (1970) 8.
26. S. GHOSE, *ibid.* **17** (1964) 1051.
27. G. FEKLICHEV, in "Diagnosticheskie Spectri Mineralov" (Nedra, Moskow, 1977).
28. I. KISTOV, in "Mineralogia" (Nauka i Izskustwo, Sofia, 1957).
29. H. ADLER and P. KERR, *Amer. Mineral.* **48** (1963) 839.
30. L. MIRKIN, in "Rentgenostructurnii Analiz-Inducirovanie Poroshkovih Rentgenogramm" (Nauka, Moskow, 1981).
31. J. RABO, in "Zeolite Chemistry and Catalysis" (ACS. Monograph, Washington, 1976) part 1.
32. H. IMAI, T. TAKAGAWA and N. KAMIDE, *J. Catal.* **106** (1987) 394.
33. P. TARTE, in "Proceedings of the International Conference on Physics of Non-Crystalline Solids" (1965) p. 549.
34. P. GIGUERE and K. HARVEY, *Can. J. Chem.* **34** (1955) 798.
35. Y. TAKITA and J. LUNSFORD, *J. Phys. Chem.* **83** (1979) 683.
36. H. MIYATA, M. WAKAMIYA and I. KIBOKAWA, *J. Catal.* **34** (1974) 117.
37. J. LERCHER, C. COLOMBIER, H. VINEC and H. NOLLER, in "Catalysis by Acids and Bases" eds, B. Imelik, C. Maccache, G. Cardurier, Y. Ben Taarit and J. C. Verdine (Elsevier, Amsterdam, 1985) p. 25.

Received 25 November 1991
and accepted 11 August 1992